Transition from Transparent Aerogels to Hierarchically Porous Monoliths in Polymethylsilsesquioxane Sol-Gel System

Kazuyoshi KANAMORI*, Yasunori KODERA, Gen HAYASE, Kazuki NAKANISHI, Teiichi HANADA

Department of Chemistry, Graduate School of Science, Kyoto University, Kitashirakawa, Sakyo-ku, Kyoto 606-8502, Japan.

*Corresponding author: Kazuyoshi KANAMORI, Dr. Eng.

TEL/FAX: +81-75-753-7673, E-mail: kanamori@kuchem.kyoto-u.ac.jp

Abstract

A transition from hierarchical pore structures (macro- and mesopores) to uniform mesopores in monolithic polymethylsilsesquioxane (PMSQ, $CH_3SiO_{1.5}$) gels has been investigated using a sol-gel system containing surfactant Pluronic F127. The precursor methyltrimethoxysilane (MTMS) undergoes an acid/base two-step reaction, in which hydrolysis and polycondensation proceed in acidic and basic aqueous media, respectively, as a one-pot reaction. Porous morphology is controlled by changing the concentration of F127. Sufficient concentrations of F127 inhibit the occurrence of micrometer-scale phase separation (spinodal decomposition) of hydrophobic PMSQ condensates and

1

lead to well-defined mesoporous transparent aerogels with high specific pore volume as a result of the colloidal network formation in a large amount of solvent. Phase separation regulates well-defined macropores in the micrometer range on decreasing concentrations of F127. In the PMSQ-rich gelling domain formed by phase separation, the PMSQ colloidal network formation forms mesopores, leading to monolithic PMSQ gels with hierarchical macro- and mesopore structures. Mesopores in these gels do not collapse on evaporative drying owing to the flexible networks and repulsive interactions of methyl groups in PMSQ.

Keywords

polymethylsilsesquioxane, sol-gel, macroporous, mesoporous, aerogels, hierarchically porous gels

1. Introduction

Porous materials with various chemical compositions are widely used as adsorbents, gas storage, catalyst supports, filters, membranes, and separation media [1-6]. The representative protocols to tailor porous materials rely on foaming, soft- and hard-templating, and phase separation, all of which take place during solidification of the material from a precursor solution. The sol-gel technique, for example, is often employed to synthesize porous materials in liquid media with various pore characteristics. After multiphase structures are formed during hydrolysis and polycondensation reactions of precursor, removing the adequate phase(s) while leaving at least one solidified phase results in porous materials. In addition to the well-known ordered and disordered mesoporous materials [7], which are typically synthesized using the soft templates formed by surfactant micelles (structure-directing agents, SDA), various porous materials with hierarchical structures are becoming more important [8-13]. Fast mass transport as well as high surface area is highly expected because hierarchically porous materials possess two or more discrete size levels of pores. For the applications that require enhanced contact of external fluid with the solid surface such as in separation media and catalyst supports, in particular, materials or devices designed to have hierarchical pore structures are highly demanded.

We have designed a number of hierarchically porous materials by the sol-gel technique accompanied by phase separation to enhance the separation efficiency in high performance liquid chromatography (HPLC) [14-17]. Spinodal decomposition-type phase separation in a macroscopic scale regulates macropores typically in micrometers, through which liquid flows with a low pressure drop. Mesopores typically in nanometers are developed by Ostwald ripening [18] and soft-templating by SDA [19,20].

Of various sol-gel materials, polymethylsilsesquioxane (PMSQ, $CH_3SiO_{1.5}$) typically derived from methyltrialkoxysilanes possesses unique surface characters due to the presence of hydrophobic methyl groups as well as hydrophilic silanol groups. We, for instance, have reported that separation media composed of PMSQ can separate both polar and nonpolar molecules in normal and reversed phase modes, respectively [21,22]. Rao *et al.* also showed that porous PMSQ can supply a superhydrophobic surface with the aid of surface roughness and surface modification [23,24]. The PMSQ materials also exhibit unique mechanical properties arising from the lower cross-linking density compared to silica and less-polar methyl groups that repel each other when compressed. Aerogels with PMSQ composition are reported to show "spring-back" and bendable features without being broken [25-30]. Methylsilsesquioxane-based films (and other organotrialkoxysilane-derived films) for low-*k* applications also exhibit unique mechanical properties such as decreased elastic modulus, hardness, brittleness and

the emergence of viscoelastic properties [31-37].

In the course of spinodal decomposition induced during the sol-gel transition of PMSQ in a polar medium such as water and alcohol, we [15,21,22] and Dong *et al.* [38-40] found that well-defined macropores are formed. However, formation of monolithic gel [41] as well as the phase separation behavior is severely influenced by many factors including pH, amount and polarity of the solvent, water content, and temperature because of the hydrophobicity of the resultant networks and cyclization reactions. The cyclization reactions do not contribute to the random network formations, which are a requisite for gelation in monolith, but instead contribute to the formation of low-molecular-weight products such as polyhedral oligomeric silsesquioxanes (POSS) [42]. Only a few reports on macroporous monolithic PMSQ materials with random networks hence can be found in literatures except for those by us [15,21,22] and Dong *et al* [38-40]. In addition, PMSQ with hierarchical pore structures is hardly found. Although Dong *et al.* [38] reported that mesopores are present in the macroporous skeletons of PMSQ monolith prepared by a two-step acid/base process, no detailed and systematic research on the formation of mesopores has been done. It is also known that PMSQ condensates cannot be structured with SDA because of the absence of specific surfactant-condensates interactions, which is fundamental for mesopore formations. For these reasons, PMSQ materials with hierarchical pore structures are difficult to be prepared, regardless of their unique properties such as hydrophobicity

and mechanical flexibility.

In this research, transitions of pore structures from mesoporous to hierarchical meso/macroporous in PMSQ monolith have been investigated in the sol-gel system containing methyltrimethoxysilane (MTMS), surfactant, and urea [26-30]. This system relies on the hydrolysis of MTMS in weakly acidic media and subsequent polycondensation in weakly basic media. The pH of the hydrolyzed sol is increased by *in-situ* hydrolysis of urea. Although we firstly found this system is suitable for tailoring transparent aerogels with a unique spring-back behavior, here we also found that macropores with well-defined bicontinuous structure are regulated in the compositional range with decreased concentrations of surfactant. In addition, mesopores are formed as a result of colloidal aggregation of PMSQ particles within the relatively soft networks. The formation mechanism of porous structures is discussed.

2. Experimental

2.1 Materials

Acetic acid (denoted as HOAc), distilled water, and urea were purchased from Hayashi Pure Chemical Ind., Ltd (Japan). Surfactant poly(ethylene oxide)-*block*-poly(propylene oxide)-*block*-poly(ethylene oxide) (EO$_{106}$PO$_{70}$EO$_{106}$, Pluronic F127, M_{w} = 12600) was from BASF

(Germany). Methyltrimethoxysilane (MTMS) was obtained from Shin-Etsu Chemical Co., Ltd (Japan).

All reagents were used as received.

2.2 Synthesis Procedure

The starting compositions are listed in Table 1. In a typical synthesis, 6 mL of diluted aqueous

acetic acid (5 mM), 0.5 g of urea, and 0−1.0 g of surfactant (F127) were mixed in a glass sample bottle,

and 5 mL of MTMS was subsequently added under vigorous stirring. The molar ratios of starting

materials are MTMS:water:acetic acid:urea:F127 = 1:9.6:0.00086:0.24:0−0.0023. After the mixed

solution was continuously stirred for 30 min at room temperature, the resultant homogeneous solution

was allowed to gel at 60 °C in a closed vessel. Gelation time was 6−6.5 h for all samples, and phase

separation (if induced) and gelation were almost concurrent. The wet gel was then aged for 5 d to

complete the condensation, followed by washing with methanol for three times (more than 8 h at 60 °C

for each time) to remove the surfactant, unreacted species, *etc*. Shrinkage in the samples after aging is

listed in Table 1. The washed sample was subjected to the solvent exchange with 2-propanol for three

times in the identical way to washing.

To dry wet gels, supercritical drying and evaporative drying at ambient pressure were performed.

For supercritical drying, 2-propanol in wet gels was exchanged with supercritical carbon dioxide at

80 °C and 14 MPa in a custom-built autoclave (Mitsubishi Materials Techno Corp., Japan) followed by a

slow depressurizing to atmospheric pressure.   The samples underwent shrinkage only in a few percent during supercritical drying.   For evaporative drying under ambient pressure, 2-propanol in wet gels was slowly removed by evaporation at 40 °C for 5 d.   In this work, all the gels were supercritically dried otherwise stated, to minimize the effect of shrinkage.

2.3 Measurements

Bulk density was obtained from the weight/volume ratio of a sample.   Thermal analysis was carried out with a thermogravimetry-differential thermal analysis (TG-DTA) system (Thermoplus TG 8120, Rigaku Corp., Japan) at a heating rate of 5 °C min^{-1} under an air flow.   While morphologies of the dried gels in the micrometer range were observed with a scanning electron microscope (SEM, JSM-6060S, JEOL Ltd., Japan), those in the nanometer range were observed with field-emission SEM (FE-SEM, JSM-6700F (JEOL Ltd., Japan)).   Mercury intrusion measurements were performed with PoreMaster 60-GT (Quantachrome Instruments, USA) to characterize macropores.   Nitrogen adsorption-desorption measurements at 77 K using ASAP 2010 (Micromeritics, USA) were performed to obtain mesopore size distributions.   Samples were outgassed under vacuum at 80 °C for at least 8 h prior to each measurement.   Specific surface areas were calculated by the BET method in the relative pressure range of 0.06–0.20.   For pore size distributions, adsorption branch was used in the BJH calculation.

3. Results & Discussion

3.1   General trends: Morphologies and thermal properties

Table 1 exhibits the starting compositions with the fixed amount of aqueous acetic acid (6 mL).

Macroporous morphologies of selected samples are shown in Figure 1.   With increasing amount of

F127, macroporous morphology varies from "aggregate of particles" (M6-0), "bicontinuous" (M6-32

and -36), and to "no distinct macropores" (M6-40).   Further increase of F127 to 1.0 g allows resultant

wet gels to become more transparent; as previously reported, supercritically-dried aerogels show ~ 50 %

light transmittance (at 550 nm through 10 mm-thick samples) and > 85 % porosity [26-30].   The

bicontinuous structure results from spinodal decomposition, in which three-dimensional compositional

fluctuation grows in time.   The more coarsened structure is frozen by gelation when phase separation

starts earlier than gelation, *i.e.* phase separation tendency becomes higher.   From these observations, it

can be concluded that F127 suppresses phase separation in the PMSQ−water system by enhancing the

mutual miscibility.   In other words, morphology becomes finer with increasing amount of F127.

M6-0   M6-32   5 µm   5 µm

M6-34   M6-36   5 µm   5 µm

M6-38   M6-40   5 µm   5 µm
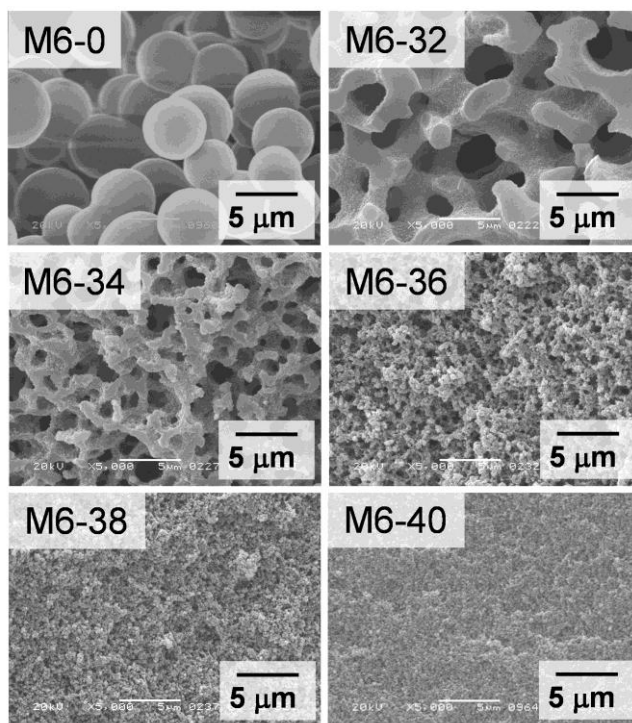
[Figure 1]

Shrinkage and bulk density show a good correlation for samples containing F127 as shown in

Table 1.   Higher shrinkage was observed with decreasing F127.   The higher shrinkage is generally

observed for more phase-separated samples because the condensates, which are more closely located

each other after the onset of phase separation, continue to undergo local condensations even after

gelation.   In addition, since a weak hindrance of silanol groups by hydrogen bonding with F127

molecules was observed [27], increasing amount of F127 with respect to MTMS may slightly hinder the

local condensations, leading to the lower shrinkage.

In Figure 2, the relationship between starting composition and morphology is presented.   Without

F127 (on the left side of the triangle), morphology changes from no distinct macropores, bicontinuous,

10

to aggregate of particles with increasing amount of water.   This is attributed to the enhanced phase

separation tendency due to increased repulsive interaction between water and less-polar MTMS-derived

condensates and to prolonged gelation.   The phase separation tendency becomes lower with increasing

F127, and the bicontinuous structure with well-defined macropores forms in a relatively small

compositional area.
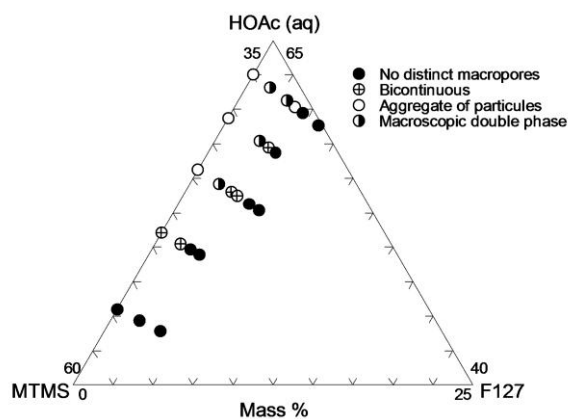
[Figure 2]

Thermal analysis by TG-DTA was carried out to confirm that the surfactant is thoroughly

extracted through the solvent exchange processes.   For as-dried gels, since no exothermic peaks

accompanied by a weight loss can be found except for the thermal decomposition of methyl groups at ~

400 °C [43], all of the surfactant are removed through the washing and solvent-exchanging processes

before drying.

3.2   Transition of hierarchical porous structures in PMSQ networks

3.2.1   In the low surfactant concentration region

Next we show the transition of pore structures with varied starting compositions.   Figure 3 represents the porous structures in the nanometer range of the samples prepared with relatively low concentrations of F127 (up to 0.34 g).   Nitrogen adsorption-desorption isotherms and BJH pore size distributions, and obtained parameters are shown in Figure 4 and Table 1.   Mesopore size and volume become larger with increasing amount of F127, namely, with the decreasing phase separation tendency. Values of BET surface area, however, are nearly constant between M6-32 and -34.   This is attributed to the fact that micropores, which had been penetrated with F127 before washing [28,44,45] and contribute surface area the most, are not changed.   Note that in Figure 3, no mesopores can be found in M6-0; however, mesopores with *ca.* 10 nm in diameter are confirmed in-between primary particles in M6-32 and -34.   The BJH data given in Figure 4 also confirms that small pores with mainly 7–10 nm are present.   As discussed later in greater detail, these mesopores are formed through the aggregation of PMSQ colloidal condensates, which takes place in one of the separated phases mainly composed of the colloidal condensates and solvents.   The mesopore size and volume change in accordance with the compositions inside the separated phase.
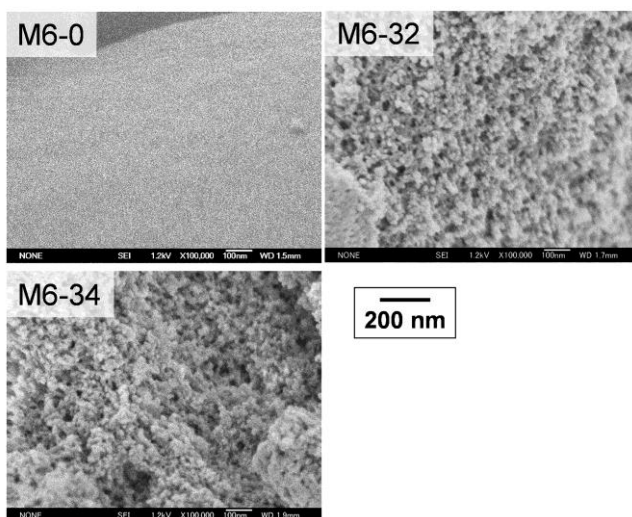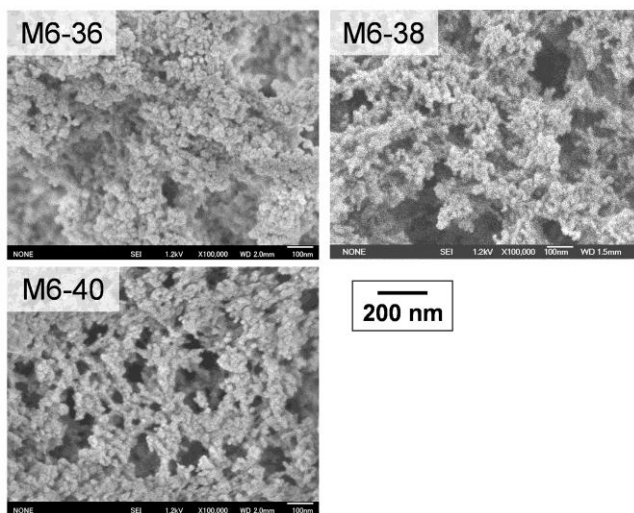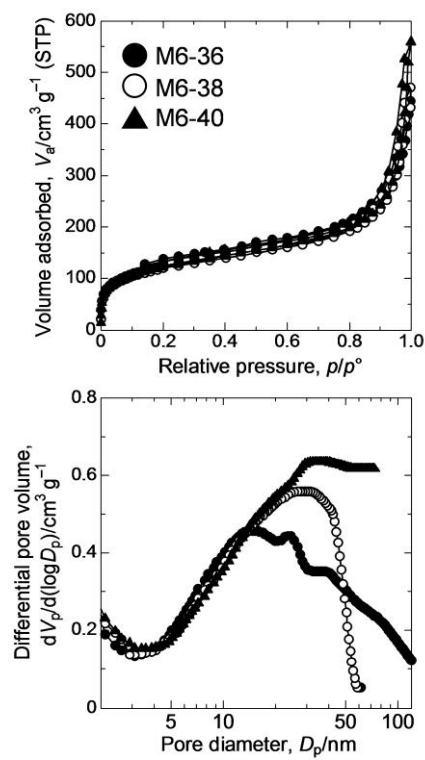
[Figure 3]
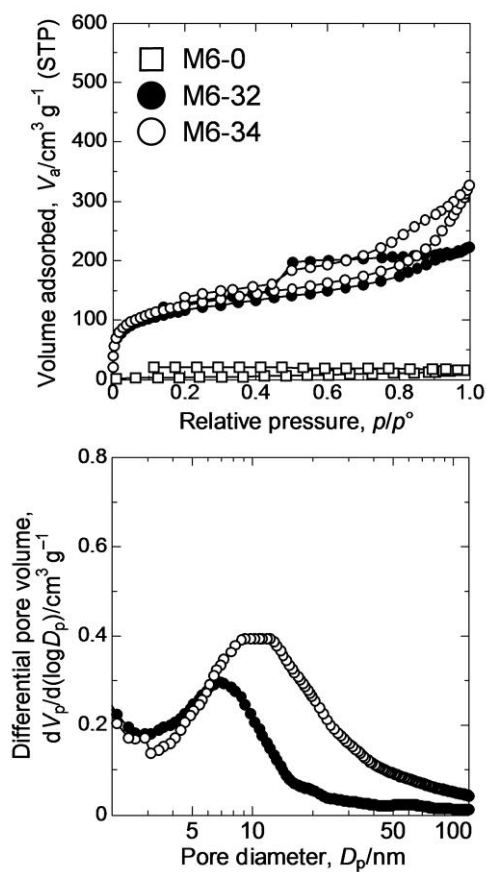
[Figure 4]

3.2.2　In the middle surfactant concentration region

13

With increasing F127 up to 0.40 g, the phase separation tendency is more declined and macropores become smaller as shown in Figure 1. Figure 5 shows the porous structures in the nanometer range of M6-36, -38, and -40. In this region, inter-particles pores and heterogeneity induced by phase separation become in the similar scale. In M6-36, macropores resulted from phase separation are in the micrometer scale (Figure 1 and 5), which are considerably larger than inter-particles mesopores. In M6-38 and -40, macropores are in the order of hundred nanometers (Figure 5). From nitrogen adsorption-desorption measurements exhibited in Figure 6, the size of the inter-particles pores changes from *ca.* 15 nm (M6-36), 30 nm (M6-38), and to 40 nm (M6-40). In samples M6-38 and -40, the nitrogen adsorption uptakes do not saturate at the relative pressure close to unity, indicating that capillary condensation still continues at $p/p^{\circ} \sim 1$ due to the coarse structures in the submicron scale developed by phase separation. The BJH pore volume increases with increasing F127 and almost constant BET specific surface area is confirmed in this compositional region as well.

[Figure 5]

[Figure 6]

It is known that spinodal decomposition starts with an uphill diffusion of components without

distinct interfaces and with various wavelengths of compositional fluctuation in the early stage [46,47].

15

The multi-phase domains grow in size in accordance with a dominant wavelength and simultaneously interfaces become more distinct in the middle stage. Finally, the domains with distinct interfaces further grow in size to reduce interfacial area. In samples M6-36, -38, and -40, since the macroporous structure is frozen in the early stage of spinodal decomposition when interfaces between the phases are still indistinct and various wavelengths of fluctuation are allowed, the overall porous structure is largely affected by the compositional fluctuation to give the heterogeneity in a few tens to hundreds nanometers. Accordingly, the inter-particles mesopores are disturbed and become coarser as later shown in Figure 10.

### 3.2.3   In the high surfactant concentration region

While the samples with less than 0.40 g of F127 are all opaque, those with more than 0.60 g become more transparent with increasing concentration of F127 (Figure 7) because phase separation is more highly suppressed. Figures 8 and 9 show the porous structures and pore size distributions. With increasing amount of F127, the BJH pore diameters become smaller from *ca.* 60 nm (M6-60), 35 nm (M6-80), and to 30 nm (M6-100). The BET specific surface area and BJH specific pore volume increase drastically up to 623 $m^2 g^{-1}$ and 3.3 $cm^3 g^{-1}$, respectively, because of the increased fraction of mesopores (see Table 1). Pore structure becomes more uniform in the nanometer scale and no distinct macropores by phase separation are confirmed.

In the course of polycondensation of MTMS, hydrophilic (or amphiphilic) oligomers turn into

16

hydrophobic polymers by consuming silanol groups. Phase separation is effectively suppressed

through the attractive interaction between the oligomers and EO unit of the surfactant by hydrogen

bonding, and then through the weak hydrophobic interaction between polymers and PO unit [48,49].

The EOPOEO surfactant is more likely to control the hydrophilic/hydrophobic nature of the condensates

by adsorbing on the surfaces, rather than to direct well-defined mesopores through the

structure-direction mechanism as well-known in mesoporous silica systems such as SBA-15 [50].

Since the attractive interaction of methylsiloxane networks with EOPOEO-type surfactant [51], as well

as with ionic surfactant [52,53], is not strong, disturbance of ordering of mesopores is reported in

co-gelation systems of organotri- and tetraalkoxysilanes with an increasing organotrialkoxysilane ratio.
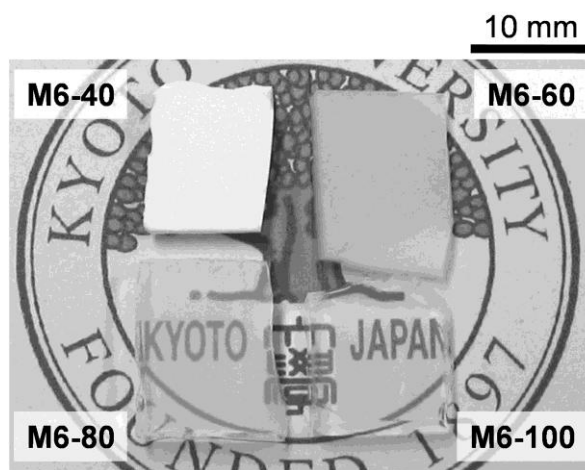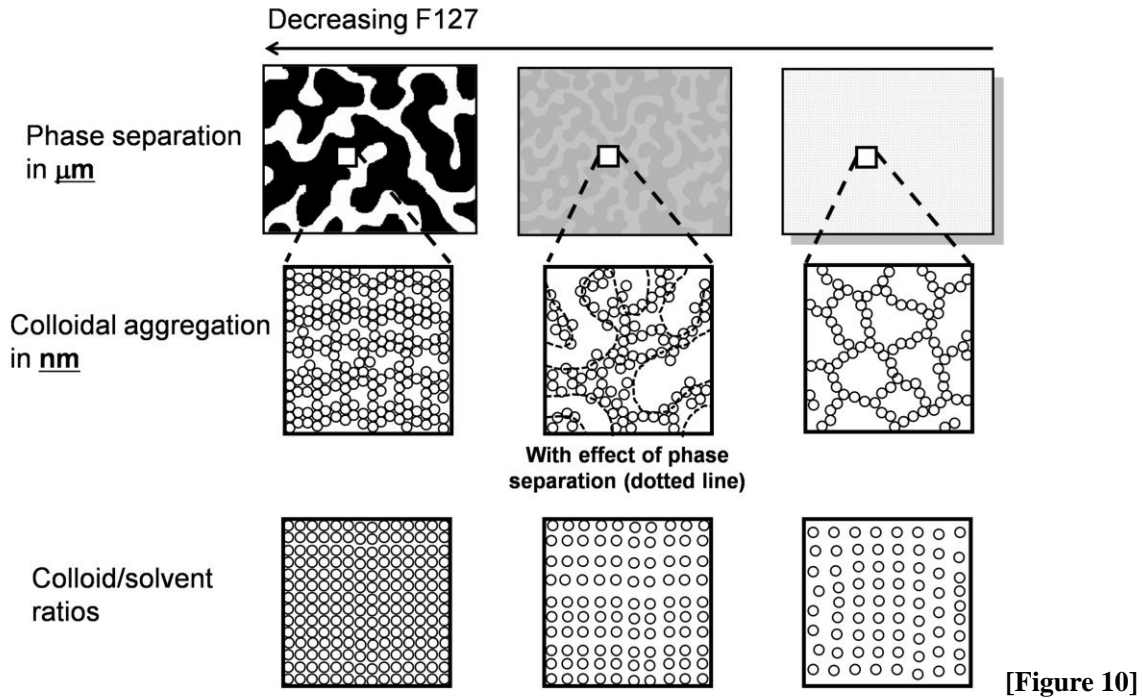

[Figure 7]

17
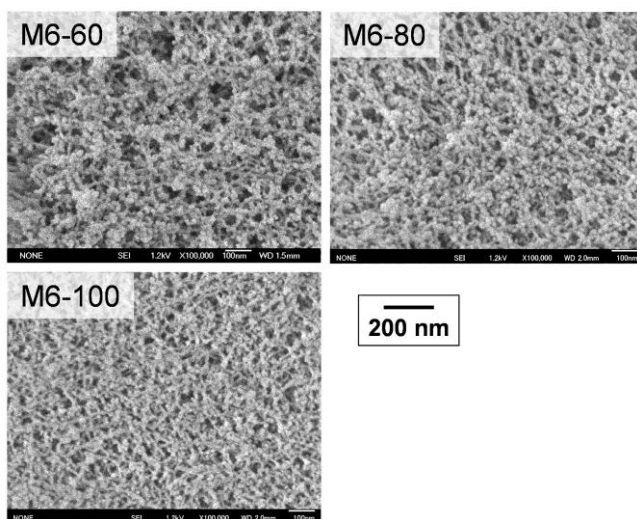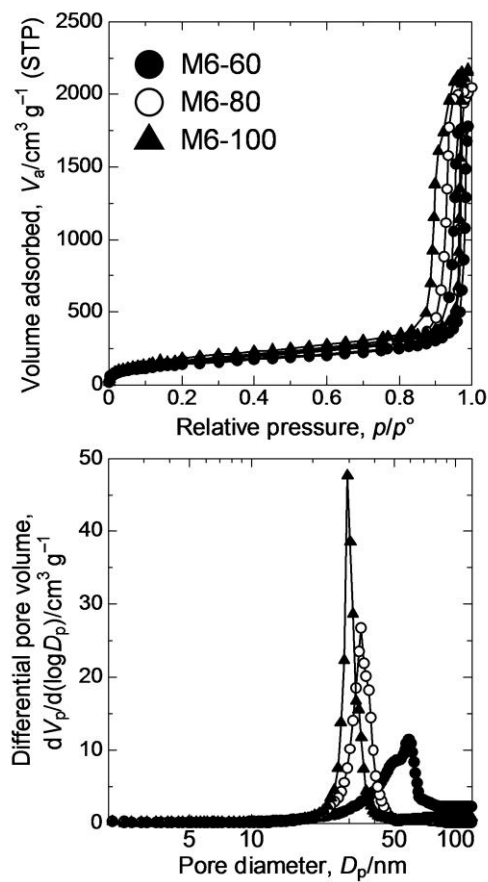
[Figure 8]

[Figure 9]

3.3. Proposed mechanism for transition of pore structures

The proposed mechanism of morphological change is illustrated in Figure 10 based on the relative timing and interplay between phase separation and colloidal aggregations. In the systems with enough concentrations of F127 (typically in M6-100), phase separation is completely suppressed and only mesopores form as a result of aggregations of PMSQ colloids, as shown in the right column of Figure 10. The PMSQ oligomers grow in size and form colloids in the course of polycondensation. The colloids, which are 10–20 nm in diameter judged from FE-SEM images, connect to each other by forming new siloxane bonds on the surfaces through collision induced by the Brownian motion. Since the amount of solvent is high in this case (because no phase separation occurs, as discussed later), uniform mesopores with high pore volume form, which fact can be confirmed in the nitrogen adsorption data given in Figure 9 and Table 1. In this compositional region, we have already reported that the transparent aerogels with high porosity can be obtained [26-30].

Decreasing F127 ←

Phase separation in μm

Colloidal aggregation in nm

With effect of phase separation (dotted line)

Colloid/solvent ratios

[Figure 10]

With decreasing F127, macroscopic phase separation becomes to develop and PMSQ colloids are concentrated in one of the separated phases, resulting in the lower volume of mesopores; the decrease of mesopore volume can be explained in a way that the solvent is extruded from the PMSQ-rich gelling phase to the solvent-rich fluidic phase in the course of phase separation.   The mesopore size becomes larger particularly in M6-60 and M6-40 with decreased F127 due to the disturbance by phase separation. This situation is illustrated in the middle column of Figure 10.

Finally, macropores become more distinct and larger on further decreasing F127.   The disturbance of the colloidal aggregation by phase separation becomes weaker because the scale of phase separation far exceeds that of the colloidal aggregation (typically in M6-34 and -32).   Also, the amount

20

of solvent in the gelling phase becomes smaller due to the higher phase separation tendency. The

mesopore size and volume consequently become smaller and lower as illustrated in the left column of

Figure 10. It is also noticeable that no mesopores (and micropores) are left in the sample M6-0. At

the onset of phase separation, the PMSQ oligomers coagulate to form dense networks because the

oligomers are still small and the gelling phase leaves enough fluidity to allow the densification.

3.4. Hierarchical pore structures in PMSQ

Hierarchical pore structures with well-defined macropores and mesopores are obtained in M6-32

and -34 in the present system. From mercury intrusion and nitrogen adsorption-desorption

measurements, the samples M6-32 and -34 possess 2.1 and 0.77 μm of well-defined macropores and 7

and 10 nm of mesopores with relatively wide distributions, respectively. (Note that mercury intrusion

on other samples was not successful because the gels shrank by the applied pressure of mercury.) Dong

et al. studied the sol-gel reaction and pore formation of PMSQ by an acid/base two-step reaction in the

smaller amount of solvent without surfactant [39]. They discussed that the size and aggregation

mechanism of clusters, which are strongly dependent on the duration of hydrolysis in the acidic media,

influences the mesopore properties. The tendency of reducing mesopores with the enhancement of

phase separation tendency is consistent with our results. By contrast, a one-step reaction in strong

acidic media [21] leads to PMSQ gels only with micropores [41,51,54]. The nitrogen

21

adsorption-desorption measurements give type I isotherms, which cannot be found in the samples

prepared by the two-step process.   Weakly cross-linked networks consisting of less-branched oligomers

formed under acidic conditions [55] more effectively expel solvent in the course of phase separation and

are more easily reorganized into the dense networks.   No mesopores are thereby left in the case of the

one-step reaction in an acidic solution, and micropores remain as interstices of networks formed by the

reaction-limited cluster-cluster aggregation (RLCA) mechanism [56].   In a one-step base-catalyzed

system, Loy *et al.* also found some mesoporosity in the PMSQ materials [41] presumably because the

vigorous development of colloidal networks in basic media generates inter-particles mesopores.

However, the detailed pore structures and characteristics are unknown from the literature because no

systematic research has been done.   We show here the acid/base two-step process is suitable for

tailoring hierarchically porous structures in PMSQ, and the mesoporosity is varied dependent on the

phase separation tendency.

3.5.   Comparison between supercritical drying and evaporative drying

It is well-known that silica gels prepared by sol-gel shrink by a few tens percent in many cases and

pores are fully or partially collapsed in the course of drying due to the capillary pressure by the

evaporating solvent [57].   On the other hand, our previous research revealed that for PMSQ alcogels

(aerogel precursors immersed in alcohol solvent), pore structures do not change during evaporative

drying due to high flexibility and repulsion between the methyl groups [26-30]. In more detail, the

compliant gels temporarily shrink during evaporation of the solvent, and undergo "spring-back" when

the pores become empty. This spring-back behavior leads to aerogel-like xerogel monoliths in

optimized conditions. For the PMSQ gels with hierarchical pore structure synthesized in this research,

pore structures observed with SEM (shown in Figure S1 in Supporting Information) and nitrogen

adsorption-desorption isotherms (Figure S2) also exhibit pore structure within micrometer and

nanometer ranges are almost equivalent regardless of the drying techniques. This behavior is in

contrast to the case of silica gels in which large shrinkage occurs, and demonstrates that the spring-back

taking place in the PMSQ is advantageous in preserving porosity.

Conclusions

Pore structure changes in organic-inorganic hybrid PMSQ gels have been investigated using the

trifunctional precursor MTMS via an acid/base two-step sol-gel reaction under the presence of nonionic

surfactant Pluronic F127. The resultant PMSQ gels show a transition from hierarchically pore

structures with well-defined macropores and mesopores, to uniform mesopores with increasing

concentration of F127. Macropores form by phase separation (spinodal decomposition) of the PMSQ

condensates and the tendency of phase separation can be controlled by the concentration of F127.

23

Mesopores form through the aggregation of PMSQ colloids.   The size and volume of mesopores can also be varied by the concentration of F127 since mesopore characteristics are mainly defined by the amount of solvent in which the colloidal aggregation occurs, and the amount of solvent changes with the progress of phase separation.   In the later stage of phase separation, namely, when the gelling phase contains less amount of solvent, mesopore structures become finer and mesopore volume lower.   In the case where macroscopic phase separation is effectively suppressed, transparent aerogels containing well-defined mesopores with high specific pore volume are obtained.   The phase-separating structure gives a strong influence on the colloidal aggregation in the case where the length scales of both mechanisms are similar.

Comparison between hierarchical porous PMSQ gels dried in a supercritical condition and those dried by evaporation has also been made.   Pore properties of gels dried by both techniques are close owing to the spring-back behavior during evaporative drying resulting from the flexible networks and repulsive methyl groups, which is in contrast to the case of silica gels.   Together with the controlled pore formation in the present system, the easy drying process allows a better control of mesopore properties and extended applications are highly expected particularly to separation media, in which a combination of macropores and mesopores are highly important.

Ackowledgement

References

[1] A.F. Ismail, L.I.B. David, J. Membr. Sci. 193 (2001) 1-18.

[2] J. Banhart, Prog. Mater. Sci. 46 (2001) 559-632.

[3] S. Kitagawa, R. Kitaura, S. Noro, Angew. Chem. Int. Ed. 43 (2004) 2334-2375.

[4] A.R. Studart, U.T. Gonzenbach, E. Tervoort, L.J. Gauckler, J. Am. Ceram. Soc. 89 (2006) 1771-1789.

[5] X.-Y. Yang, Y. Li, A. Lemaire, J.-G. Yu, B.-L. Su, Pure Appl. Chem. 81 (2009) 2265-2307.

[6] F. Svec, J. Chromatogr. A 1217 (2010) 902-924.

[7] G.J.A.A. Soler-Illia, C. Sanchez, B. Lebeau, J. Patarin, Chem. Rev. 102 (2002) 4093-4138.

[8] P. Yang, T. Deng, D. Zhao, P. Feng, D. Pine, B.F. Chmelka, G.M. Whitesides, G.D. Stucky, Science 282 (1998) 2244-2246.

[9] G. Zhao, P. Yang, B.F. Chmelka, G.D. Stucky, Chem. Mater. 11 (1999) 1174-1178.

[10] T. Sen, G.J.T Tiddy, J.L. Casci, M.W. Anderson, Angew. Chem. Int. Ed. 42 (2003) 4649-4653.

[11] T. Sen, G.J.T. Tiddy, J.L. Casci, M.W. Anderson, Chem. Mater. 16 (2004) 2044-2054.

[12] D. Brandhuber, V. Torma, C. Raab, H. Peterlik, A. Kulak, N. Hüsing, Chem. Mater. 176 (2005) 4262-4271.

[13] Z.-Y. Yuan, B.-L. Su, J. Mater. Chem. 16 (2006) 663-677.

[14] K. Nakanishi, J. Porous Mater. 4 (1997) 67-112.

[15] K. Nakanishi, K. Kanamori, J. Mater. Chem. 15 (2005) 3776-3786.

[16] K. Nakanishi, Bull. Chem. Soc. Jpn. 79 (2006) 673-691.

[17] K. Nakanishi, N. Tanaka, Acc. Chem. Res. 40 (2007) 863-873.

[18] K. Nakanishi, R. Takahashi, T. Nagakane, K. Kitayama, N. Koheiya, H. Shikata, N. Soga, J. Sol-Gel

Sci. Technol. 17 (2000) 191-210.

[19] K. Nakanishi, Y. Kobayashi, T. Amatani, K. Hirao, T. Kodaira, Chem. Mater. 16 (2004) 3652-3658.

[20] T. Amatani, K. Nakanishi, K. Hirao, T. Kodaira, Chem. Mater. 17 (2005) 2114-2119.

[21] K. Kanamori, H. Yonezawa, K. Nakanishi, K. Hirao, H. Jinnai, J. Sep. Sci. 27 (2004) 874-886.

[22] K. Kanamori, K. Nakanishi, T. Hanada, J. Sep. Sci. 29 (2006) 2463-2470.

[23] A.V. Rao, S.D. Bhagat, S.S. Latthe, D.Y. Nadargi, H. Hirashima, V. Ganesan, J. Colloid Interface

Sci. 332 (2009) 484-490.

[24] D.Y. Nadargi, S.S. Latthe, H. Hirashima, A.V. Rao, Microporous Mesoporous Mater. 117 (2009)

617-626.

[25] A.V. Rao, S.D. Bhagat, H. Hirashima, G.M. Pajonk, J. Colloid Interface Sci. 300 (2006) 279-285.

[26] K. Kanamori, M. Aizawa, K. Nakanishi, T. Hanada, Adv. Mater. 19 (2007) 1589-1593.

[27] K. Kanamori, M. Aizawa, K. Nakanishi, T. Hanada, J. Sol-Gel Sci. Technol. 48 (2008) 172-181.

[28] K. Kanamori, K. Nakanishi, T. Hanada, J. Ceram. Soc. Jpn. 117 (2010) 1333-1338.

[29] K. Kanamori, K. Nakanishi, Chem. Soc. Rev. in press. (DOI: 10.1039/C0CS00068J)

[30] K. Kanamori, J. Ceram. Soc. Jpn. in press.

[31] J. Malzbender, G. de With, J. Non-Cryst. Solids 265 (2000) 51-60.

[32] A.M. Padovani, L. Rhodes, L. Riester, G. Lohman, B. Tsuie, J. Conner, S.A.B. Allen, P.A. Kohl, Electrochem. Solid-State Lett. 4 (2001) F25-F28.

[33] L.-H. Lee, W.-C. Chen, W.-C. Liu, J. Polym. Sci., Part A: Polym. Chem. 40 (2002) 1560-1571.

[34] S. Kim, Y. Toivola, R.F. Cook, K. Char, S.-H. Chu, J.-K. Lee, D.Y. Yoon, H.-W. Rhee, J. Electrochem. Soc. 151 (2004) F37-F44.

[35] A.J. Atanacio, B.A. Latella, C.J. Barbé, M.V. Swain, Surf. Coat. Technol. 192 (2005) 354-364.

[36] J.Q. Zhang, A. Matsuda, H. Muto, M. Sakai, Key Eng. Mater. 317-318 (2006) 317-322.

[37] H.W. Ro, E.S. Park, C.L. Soles, D.Y. Yoon, Chem. Mater. 22 (2010) 1330-1339.

[38] H. Dong, M.A. Brook, J.D. Brennan, Chem. Mater. 17 (2005) 2807-2816.

[39] H. Dong, J.D. Brennan, Chem. Mater. 18 (2006) 541-546.

[40] H. Dong, J.D. Brennan, Chem. Mater. 18 (2006) 4176-4182.

[41] D.A. Loy, B.M. Baugher, C.R. Baugher, D.A. Schneider, K. Rahimian, Chem. Mater. 12 (2000) 3624-3632.

[42] G. Li, L. Wang, H. Ni, C.U. Pittman Jr., J. Inorg. Organomet. Polym. 11 (2001) 123-154.

[43] K. Kamiya, T. Yoko, K. Tanaka, M. Takeuchi, J. Non-Cryst.Solids 121 (1990) 182-187.

[44] R. Ryoo, C.H. Ko, M. Kruk, V. Antochshuk, M. Jaroniec, J. Phys. Chem. B 104 (2000) 11465-11471.

[45] M. Kruk, M. Jaroniec, C.H. Ko, R. Ryoo, Chem. Mater. 12 (2000) 1961-1968.

[46] J.W. Cahn, J. Chem. Phys. 42 (1965) 93-99.

[47] T. Hashimoto, M. Itakura, H. Hasegawa, J. Chem. Phys. 85 (1986) 6118-6128.

[48] S. Yang, P.A. Mirau, C.-S. Pai, O. Nalamasu, E. Reichmanis, E.K. Lin, H.-J. Lee, D.W. Gidley, J. Sun, Chem. Mater. 13 (2001) 2762-2764.

[49] P.A. Mirau, S. Yang, Chem. Mater. 14 (2002) 249-255.

[50] D. Zhao, J. Feng, Q. Huo, N. Melosh, G.H. Fredrickson, B.F. Chmelka, G.D. Stucky, Science 279 (2002) 548-552.

[51] N. Hüsing, D. Brandhuber, P. Kaiser, J. Sol-Gel Sci. Technol. 40 (2006) 131-139.

[52] A.R. Balkenende, F.K. de Theije, J.C.K. Kriege, Adv. Mater. 15 (2003) 139-143.

[53] M. Matheron, T. Gacoin, J.-P. Boilot, Soft Matter 3 (2007) 223-229.

[54] S. Laschober, M. Sulyok, E. Rosenberg, J. Chromatogr. A. 1144 (2007) 55-62.

[55] C.J. Brinker, G.W. Scherer, J. Non-Cryst.Solids 70 (1985) 301-322.

[56] C. J. Brinker, G. W. Scherer, Sol-Gel Science: The Physics and Chemistry of Sol-Gel Processing,

Academic Press, San Diego, 1990, pp.194-203.

[57] G.W. Scherer, J. Am. Ceram. Soc. 73 (1990) 3-14.

Table

Table 1 Stating compositions and obtained mesopore properties[a]

Notation	F127 /g	Shrinkage during aging (%)	Bulk density /g cm^{-3}	Mesopore size /nm	BJH Specific pore volume[b] /cm^3 g^{-1}	BET Specific surface area /m^2 g^{-1}
M6-0	0	3	0.33	−	0.029	14
M6-32	0.32	25	0.42	7	0.22	414
M6-34	0.34	18	0.42	10	0.37	446
M6-36	0.36	12	0.35	~ 20	0.52	444
M6-38	0.38	11	0.32	30	0.52	428
M6-40	0.40	10	0.30	37	0.61	437
M6-60	0.60	4	0.28	~ 55	2.65	513
M6-80	0.80	4	0.28	35	3.08	576
M6-100	1.00	3	0.22	30	3.30	623

[a] Other components; MTMS 5 mL, 5 mM HOAc 6 mL, and urea 0.50 g.

[b] Pores between 2 and 100 nm in size are considered for evaluation of BJH pore volume.

Figure legends

Figure 1 Micrometer-scale macroporous structures observed with SEM. It is confirmed that macropores become smaller with increasing amount of F127 (from M6-0 (0 g) to M6-40 (0.40 g)). All images are in the identical magnification.

Figure 2 Relationship between starting compositions (in mass %) and obtained macroscopic morphologies. Macroscopic morphologies become coarser with increasing aqueous acetic acid solution or with decreasing F127.

Figure 3 Nanometer-scale mesoporous structures observed by FE-SEM. While no mesopores are observed in the macropore walls of M6-0, small mesopores (7–10 nm) are formed in the walls of M6-32 and -36. For detailed mesopore properties, see Figure 4 and Table 1.

Figure 4 Nitrogen adsorption-desorption isotherms for the samples shown in Figure 3. While M6-0 shows virtually no adsorption (no micro- and mesopores), samples M6-32 and -34 possess a small fraction of mesopores.

Figure 5 Nanometer-scale mesoporous structures observed by FE-SEM. Mesopores become larger and macropores induced by phase separation becomes smaller with increasing amount of F127. Macropores in M6-38 and -40 are in the submicron scales. For detailed mesopore properties, see Figure 6 and Table 1.

Figure 6 Nitrogen adsorption-desorption isotherms for the samples shown in Figure 5. In this compositional region, mesopore size becomes larger since the formation of mesopores is influenced by compositional fluctuations induced by phase separation.

Figure 7 A change in the appearance of the samples with increasing amount of F127. The samples with less amount of F127 than M6-40 are all opaque due to the presence of large-scale structures developed by phase separation. The samples become more transparent with increasing amount of F127 because the large-scale structures are eliminated owing to the suppression of phase separation. In M6-80 and -100 particularly possess the properties similar to so-called aerogels (high transparency and porosity). The thicknesses of the samples are *ca.* 3.5 mm.

Figure 8 Nanometer-scale mesoporous structures observed with FE-SEM. Mesopores become smaller and macropores become fewer with increasing amount of F127. Since virtually no macropores but only mesopores are present in the samples M6-80 and -100, the samples become highly transparent as shown in Figure 7. For detailed mesopore properties, see Figure 9.

Figure 9 Nitrogen adsorption-desorption isotherms of the samples shown in Figure 8. In this compositional region, mesopore size becomes smaller since the effect of compositional fluctuations by macroscopic phase separation becomes weaker. In samples M6-80 and -100, well-defined mesopores with sharp distributions are confirmed.

Figure 10 Schematic illustrations showing how the mesopore structure develops in parallel with phase separation. Basically, the mesopore size and volume tend to become smaller with the progress of phase separation because more solvent is extruded from the gelling phase and the aggregation of PMSQ colloids takes place in the smaller amount of solvent (from right to left). When no macroscopic phase separation occurs (right column), the colloidal aggregation occurs in a large amount of solvent. The mesopore volume is consequently large and the mesopores size distribution is sharp. With the progress of phase separation, since the length scales of phase separation and colloidal aggregation become closer, mesopores are disturbed by phase separation and larger and less-uniform mesopores form (middle column). With further progress of phase separation, the colloidal aggregation takes place without an effect of phase separation, and mesopore size and volume become smaller because of the high concentration of colloids in the separated phase (left).

Supplementary content for

Transition from transparent aerogels to hierarchically porous monoliths in polymethylsilsesquioxane sol-gel system

Kazuyoshi KANAMORI*, Yasunori KODERA, Gen HAYASE, Kazuki NAKANISHI, Teiichi HANADA

Department of Chemistry, Graduate School of Science, Kyoto University, Kitashirakawa, Sakyo-ku, Kyoto 606-8502, Japan.

*To whom correspondence should be addressed.   E-mail: kanamori@kuchem.kyoto-u.ac.jp
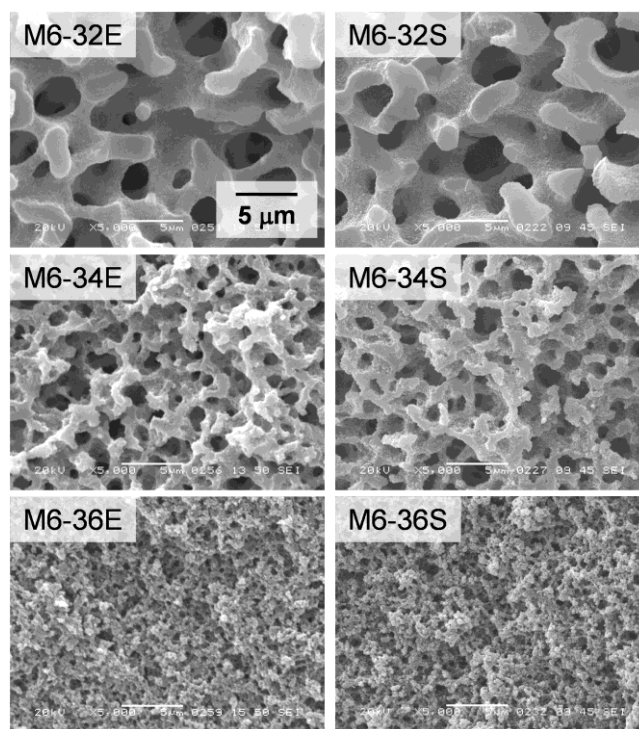
Figure S1   Comparison of macroporous structure in the samples obtained by evaporative drying at ambient pressure (E) and supercritical drying (S).   Both samples represent similar morphology, showing an ignorable shrinkage in evaporative drying.   All figures are at the identical magnification.
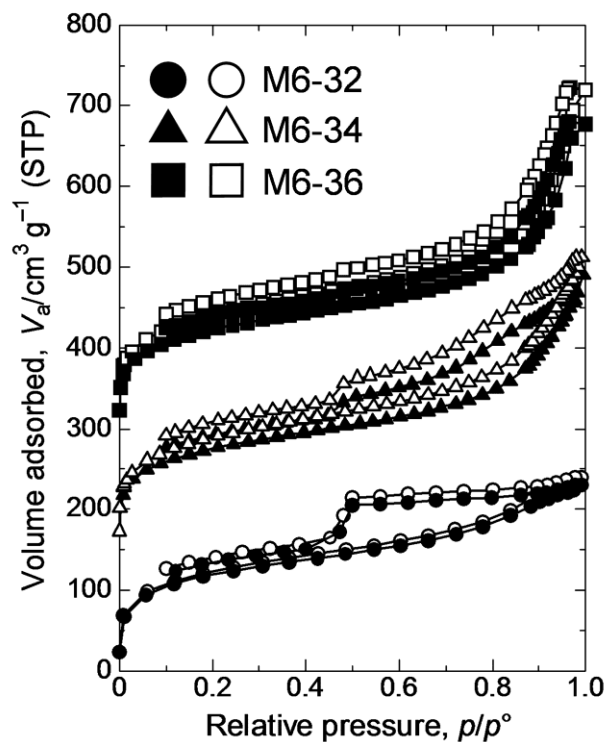
Figure S2 Comparison of nitrogen adsorption-desorption isotherms on the samples obtained by supercritical drying (closed symbols) and ambient pressure drying (open symbols).   Samples derived from both drying techniques show the similar porosity in micro- and mesopore regions as well as macropores.